ELSEVIER

Current Opinion in Colloid and Interface Science 9 (2004) 53–58

Current Opinion in COLLOID and INTERFACE SCIENCE

www.elsevier.com/locate/cocis

Competition between condensation of monovalent and multivalent ions in DNA aggregation

Yoram Burak*, Gil Ariel, David Andelman

School of Physics and Astronomy, Raymond and Beverly Sackler Faculty of Exact Sciences, Tel Aviv University, Tel Aviv 69978, Israel

Abstract

We discuss the distribution of ions around highly charged PEs when there is competition between monovalent and multivalent ions, pointing out that in this case the number of condensed ions is sensitive to short-range interactions, salt and model-dependent approximations. This sensitivity is discussed in the context of recent experiments on DNA aggregation, induced by multivalent counterions such as spermine and spermidine.

Keywords: DNA; Multivalent ions; Spermine

1. Introduction

Despite extensive theoretical and experimental research, polyelectrolyte (PE) solutions are relatively poorly understood compared to their neutral counterparts [1]. The main difficulty in their theoretical treatment arises from the long-range nature of electrostatic interactions between the charged groups along the PEs. Another major difficulty arises in highly charged PEs due to their coupling with the surrounding ionic solution, which is difficult to treat theoretically, since one cannot simply trace over the ionic degrees of freedom via the linearized Debye–Hückel theory.

In this paper we address the distribution of ions near highly charged PEs, concentrating on the case where more than one counterion species is present in the solution. We point out that the number of condensed ions is then highly sensitive to various parameters such as short-range interactions, salt concentration and model-dependent approximations—even at low concentrations of salt. In contrast, in solutions with only one type of counterion these parameters are important at high salt concentrations, e.g. in the ion-dependent solubility of proteins; at lower salt concentrations, typically up to 100 mM, their influence on ion condensation is weak.

After illustrating the above points using a simple example (Section 2), we discuss the competition between monovalent and multivalent ions in the context of DNA aggregation (Section 3), concentrating in particular on the role played by short-range interactions in the dilute (non-aggregated) phase. In Section 4 we discuss qualitatively the dependence on salt concentration of the number of condensed ions. For this purpose we use a simplified two-phase model similar to Manning's model.

2. Condensation on a single polyelectrolyte chain

Let us consider first the distribution of ions near a single PE, i.e. taking the limit of infinite dilution for the PE solution. Let us assume also that the PE is uniformly charged with a charge per unit length equal to ρ. Suppose first that there is only one type of counterions in the system.

When there is no salt in the solution only some of the ions remain bound to the PE, while the others escape to infinity. The number of bound ions, per unit length, is given by the well-known formula obtained from Manning condensation theory [2]:

$$\rho_b = \begin{cases} \frac{1}{z}(\rho - \rho^*), & \rho > \rho^* \\ 0 \quad , & \rho < \rho^* \end{cases} \tag{1}$$

where $\rho^* = 1/(z l_B)$ and $l_B = e^2/(\varepsilon k_B T)$ is the Bjerrum length, z is the counterion valency, e is the unit charge,

*Corresponding author.
E-mail address: yorambu@post.tau.ac.il (Y. Burak).

1359-0294/04/$ - see front matter © 2004 Elsevier Ltd. All rights reserved.
doi:10.1016/j.cocis.2004.05.002

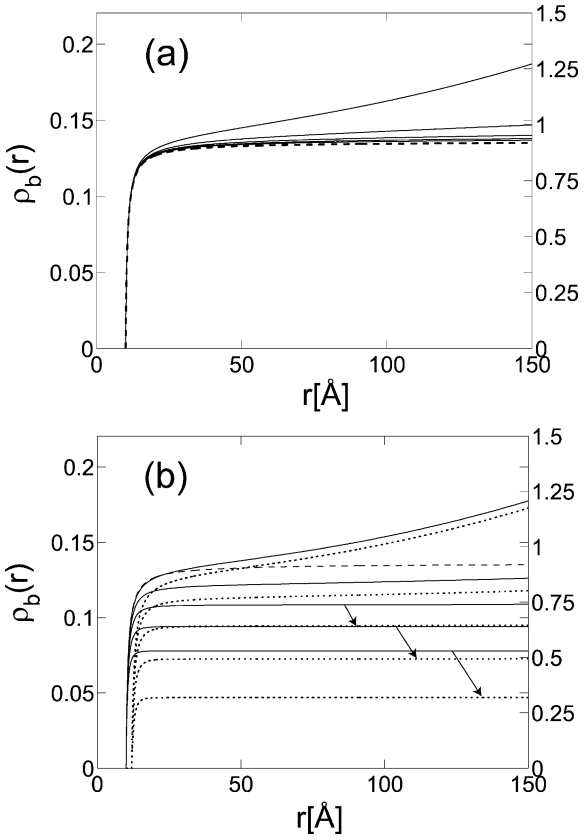

Fig. 1. Accumulated number of four-valent counterions, $\rho_b(r)$, up to a distance r from DNA, modeled as a uniformly charged cylinder of radius 10 Å: In (a), with only 4:1 salt of concentrations 0.01, 0.1, 1, 10 and 100 mM (solid lines). The limiting case of no salt (only four-valent counterions) is also shown (dashed line). In (b) 10 mM of 1:1 salt is also present in the solution (solid lines). Dotted lines correspond to larger four-valent counterions, having a distance of closest approach of 12 Å to the DNA (the arrows connect solid and dotted lines corresponding to the same 4:1 salt concentrations of 0.01, 0.1 and 1mM). The dashed line is the same as in part (a). The right axis in both figures shows $az\rho_b(r)$, the part of DNA charge compensated by the multivalent ions. In both parts the ion density profiles are calculated numerically using the Poisson–Boltzmann (PB) equation.

ε is the dielectric constant of the solvent and k_BT is the thermal energy. When $\rho > \rho^*$ the condensed ions partially neutralize the PE such that its effective charge per unit length is equal to ρ^*. This result is a consequence of the interplay between entropy and electrostatic energy at large ion–PE distances. Hence short-range interactions (ion–ion or ion–PE) are not expected to modify the number of condensed ions, although they may influence the distribution of the ions within the condensed layer.

The number of ions in the vicinity of the polymer is also insensitive to salt at low and moderate concentrations [3], as illustrated in Fig. 1a. The figure shows the accumulated number of multivalent ions ($z=4$) per unit length up to a distance r from a PE having roughly the parameters of DNA (charge per unit length equal to $1/(1.7\ \text{Å})$ and a radius of 10 Å), as a function of r. The ion distribution is modeled using mean field theory and calculated using the Poisson–Boltzmann (PB) equation. This is done for simplicity, while in fact correlation effects beyond mean field are important in this case since the ions are multivalent. The dashed line shows the distribution when there is no salt in the solution; as r increases the accumulated number of ions $\rho_b(r)$ approaches a constant, which is the number of condensed ions per unit length predicted in Eq. (1). When 4:1 salt is added to the solution at increasing concentrations of $c_z = 0.01$, 0.1, 1, and 10 mM (solid lines) the number of counterions close to the polymer is almost unaffected. A significant effect is seen only with $c_z =$ 100 mM.

Short-range interactions have no effect on the number of condensed ions in the limit of zero salt concentrations, and their effect remains small at low salt concentrations. For example, the effect of ion–PE dispersion forces was recently estimated for condensation of monovalent ions on DNA, using the Poisson–Boltzmann equation and the Hamaker approximation for the ion–PE dispersion interaction [4]. The effect was considerable at 1 M salt concentration, where electrostatic interactions are highly screened. However, below 100 mM, even with rather strong dispersion interactions, in the order of four times the thermal energy close to contact, the effect on ion condensation was small.

Returning to our numerical example, let us consider the situation when there is more than one type of counterion in the solution. Suppose that the solution contains monovalent (1:1) salt of concentration c_1, multivalent (z:1) salt of concentration c_z, and assume for simplicity that there is only one species of monovalent co-ions. The salt concentrations c_1 and c_z then determine the distribution of ions around the PE—such that far away from the PE concentrations of monovalent counterions, multivalent counterions and co-ions decay to c_1, c_z and $c_1 + zc_z$, respectively.

Fig. 1b shows results for monovalent salt of concentration $c_1 = 10$ mM and the same 4:1 salt concentrations as in part a (solid lines). For each value of c_z there is a distinct number of condensed multivalent ions, which depends on the multivalent salt concentration. This number is very different from the Manning prediction, Eq. (1), for a single counterion species (dashed line). The number of condensed multivalent ions is now determined not only by a balance of entropy and electrostatics, but also from the competition with the monovalent ions. Furthermore, this competition can be influenced by ion-specific short-range interactions [5] leading to a strong influence on the number of condensed ions. As a simple example, the dotted lines show results for multivalent ions that are slightly larger than the monovalent ions, having a radius of closest approach to the PE that is larger by 2 Å from that of the

Table 1
Excess of four-valent ions near DNA extracted from DNA aggregation experiments, compared with calculated values using Poisson–Boltzmann theory (PB) (treating the DNA as a cylinder of radius 10 Å) and Poisson–Boltzmann theory with short range interactions (SR)

c_1 [mM]	c_z^* [mM]	$a\rho_z^*$	$a\rho_z$ (PB)	$a\rho_z$ (SR)
2	0 ± 0.0003	0.194 ± 0.020	0.186 ± 0.005	0.191 ± 0.006
13	0.011 ± 0.002	0.191 ± 0.013	0.178 ± 0.002	0.172 ± 0.003
23	0.031 ± 0.005	0.173 ± 0.025	0.172 ± 0.002	0.163 ± 0.003
88	0.52 ± 0.05	0.135 ± 0.026	0.164 ± 0.002	0.149 ± 0.003

monovalent ones, leading to a considerable decrease in the condensation of multivalent ions. Compared to the case of identical ion sizes, the 4:1 salt concentration has to be increased by roughly an order of magnitude in order to have the same number of condensed multivalent ions.

3. Counterion competition in DNA aggregation

In Ref. [6] DNA aggregation, induced by multivalent ions, was studied experimentally. The conditions for aggregation were mapped with varying concentrations of monovalent salt, multivalent salt and DNA. These experiments provide interesting evidence for the role played by competition between different ion species. We will concentrate on experiments that were done in solutions containing the following ingredients: short (150 base pair) DNA chains of concentration c_{DNA} (base pairs per unit volume), spermine $(4+)$ of concentration c_z and monovalent salt of concentration c_1. At sufficiently high concentrations the multivalent salt mediates an attractive interaction between DNA chains, leading to aggregation of the DNA and its precipitation from the solution. For constant c_1 and with increase of c_z DNA starts to precipitate when c_z crosses a threshold value, which we denote as $c_{z,\mathrm{aggr}}$. The dependence of this threshold on c_1 and c_{DNA} was measured in Ref. [6] in great detail.

At the onset of aggregation all the DNA is still solubilized. The partitioning of multivalent ions into free and condensed ions is thus governed by their distribution around isolated DNA chains. Within the relevant experimental parameters, ion density profiles associated with different chains are decoupled from each other due to screening by salt. As a result, a linear dependence of $c_{z,\mathrm{aggr}}$ on c_{DNA} is expected theoretically [7]:

$$c_{z,\mathrm{aggr}} = c_z^* + a\rho_z^* c_{\mathrm{DNA}} \tag{2}$$

The first term on the right hand side, c_z^*, is the concentration of multivalent ions far away from the DNA chains. This quantity plays the role of the salt concentration, which determines the distribution of ions near the DNA chains. The second term is the contribution of condensed ions to the volume-averaged concentration of multivalent ions. The coefficient multiplying c_{DNA}, $a\rho_z^*$, is the excess of multivalent ions per DNA base, where $a = 1.7$ Å is the monomer length ($1e$ per a on the chain) and ρ_z^* is a spacial integral of the local excess of multivalent ions:

$$\rho_z^* = 2\pi \int \mathrm{d}r \; r\left[c_z(r) - c_z^*\right] \tag{3}$$

where $c_z(r)$ is the local concentration. We will assume that c_z^* and ρ_z^* do not depend on c_{DNA}, which is justified for sufficiently long chains for which translational entropy can be neglected [7]. Indeed, the experimental measurements of $c_{z,\mathrm{aggr}}$, as function of c_{DNA}, fall on straight lines (within experimental error bars) across several orders of magnitude of DNA and spermine concentrations. The coefficients c_z^* and $a\rho_z^*$ can be extracted from the experimental data [7] and are reproduced in Table 1.

3.1. Comparison with PB theory

Table 1 lists the concentrations of monovalent salt, c_1, multivalent salt c_z^* (extracted from the linear fit to Eq. (2)), and the excess of multivalent ions $a\rho_z^*$. The last quantity is a measure for the number of condensed multivalent ions at the onset of aggregation. Note that it is of the same order of magnitude for all four monovalent salt concentrations. However, c_z^* varies by at least four orders of magnitude. The large variation in c_z^* is a consequence of competition between monovalent and multivalent counterions: a relatively small increase in monovalent salt concentration requires a large addition of multivalent salt in order to keep the number of condensed multivalent ions constant. This point is further discussed in Section 4.

Table 1 provides simultaneous measurements of the salt concentrations (c_1, c_z^*) and the excess of condensed multivalent ions $a\rho_z^*$. Note that no particular model specifying the relation between c_1, c_z^* and $a\rho_z^*$ is assumed in Eq. (2) and the latter two quantities are obtained independently from the linear fit. This data can be used to test any particular theory used to calculate ion distributions around DNA. Such a comparison, with Poisson–Boltzmann (PB) theory, is shown in the fourth column of Table 1: for each pair of salt concentrations

(c_1, c_z^*) the excess $a\rho_z$, as calculated from PB theory, is compared with the experimental value of $a\rho_z^*$.

For the three smaller values of $c_1 = 2$, 13 and 23 mM there is a reasonable agreement with experiment (within the error bars). However, for $c_1 = 88$ mM there is a 30% deviation. The overall agreement with PB theory is surprisingly good, considering that PB theory does not work so well for bulky multivalent ions. Ion–ion correlations that are ignored in PB theory and are important with multivalent ions, tend to increase the number of bound multivalent counterions. Instead, for $c_1 = 88$ mM, the number of bound multivalent ions is decreased. We conclude that ion correlations by themselves are not the main source for deviations seen in Table 1, and short-range interactions also play a prominent role.

There are many types of short-range interactions that are not taken into account in PB theory. Spermine is a long, relatively narrow molecule, which can approach DNA at close proximity, and even penetrate the grooves at certain sites and orientations [8]. However, configurations that are close enough to the DNA are accompanied by a loss of orientational entropy. Other factors that modify the interaction of spermine with DNA, compared to simplified electrostatic models, include dispersion interactions, specific ordering of charges on the spermine and DNA, and arrangement of the surrounding water molecules.

Taking all the above parameters into account is beyond the scope of this work. Instead we demonstrate, within the framework of PB theory, that short-range interactions can influence the competition between monovalent and multivalent ions, and thereby affect the onset of aggregation in a similar way to that seen it Table 1. As a simple example (with somewhat arbitrary parameters chosen to demonstrate our point) two short-range effects are added to the PB model. We consider four-valent ions that are larger than the monovalent ones. Hence the distance of closest approach to the DNA is different for the two species. In this example these distances are taken as 9 Å for the monovalent counterions and 12 Å for the multivalent ones. In addition, we include a short-range attraction between the multivalent ions and DNA: multivalent ions gain 3 k_BT if their distance from the DNA is smaller than 15 Å. Qualitatively these are two competing effects. The first one (closer approach of monovalent ions) slows down replacement of monovalent ions by multivalent ions, while the second (short-range attraction) has the opposite effect. The balance between the two effects is different for different c_1 and c_z^*.

The last column of Table 1 shows values of $a\rho_z$ calculated using the above modified model. These values (SR) are shown next to the results of the usual Poisson–Boltzmann theory (PB) and compared with the experimental value of $a\rho_z^*$. For $c_1 = 2$ mM, ρ_z is almost the same in the two calculations. For $c_1 = 88$ mM and $c_z^* = 0.52$ mM, ρ_z is considerably decreased with the inclusion of short-range interactions, and is closer to the experimental value. Any one of the two short-range effects, by itself, results in a large discrepancy with experimental data at low salt concentrations.

We believe that the importance of competing mechanisms for a long, multivalent ion such as spermine go beyond the simple modifications to PB described above. More refined modifications include the loss of orientational entropy at close proximity to the DNA. This effect creates a short-range repulsion, whereas the correlation effect beyond mean-field is similar to a short-range attraction. Similar competing mechanisms were found in simulation of spermidine (3+) and NaCl in contact with DNA [9]. In particular, for high salt concentrations spermidine binding was considerably reduced compared to Poisson–Boltzmann theory. In the computer simulation [9] both molecular-specific interactions, the geometrical shape of the constituents and ion–ion correlations were taken into account. All these effects, and especially the geometry of spermidine, which is similar to that of spermine, were found to play an important role.

4. Two-phase model for competing species

Two-phase models have been widely used to describe the distribution of counterions around cylindrical macromolecules [2,10]. In these models ions are considered as either condensed or free. The condensed ions gain electrostatic energy due to their proximity to the negatively charged chain but lose entropy, since they are bound at a small cylindrical shell around it. For systems with more than one type of counterion Manning introduced the so-called two-variable theory [11], which is an extension of his previous model [2,3]. This model has been used to analyze condensation (single molecule collapse) of DNA molecules induced by spermine and spermidine [12,13]. In this section we present a similar model, which differs from Manning's two-variable theory in some details. Our main purpose is to explain the large sensitivity of c_z^* to changes in monovalent salt concentration. As a by-product of our analysis we compare our two-phase model with PB theory and Manning's two-variable theory.

4.1. Model details and main equations

Assume that the PE is confined within a finite cylindrical cell of area A. The free energy is then written as follows:

$$F = \rho_z \log\left(\lambda^3 \frac{\rho_z}{A_c}\right) + \rho_1 \log\left(\lambda^3 \frac{\rho_1}{A_c}\right) + \rho_z^f \log\left(\lambda^3 \frac{\rho_z^f}{A - A_c}\right) + \rho_1^f \log\left(\lambda^3 \frac{\rho_1^f}{A - A_c}\right) + \frac{1}{2}(-\rho_{\mathrm{DNA}} + z\rho_z + \rho_1)\phi \quad (4)$$

The first two terms are the entropy of bound multivalent and monovalent counterions, where ρ_z and ρ_1 are the number of condensed ions per unit length of the PE. We assume that condensed ions are bound on a cylindrical shell around the chain and take its area, for simplicity, to be:

$$A_c = \pi d^2 \quad (5)$$

where d is the radius of the PE. The length λ is included in order to have a dimensionless argument inside the logarithms, and can be chosen arbitrarily.

The next two terms are the entropy of free counterions. The numbers per unit area of free multivalent ions, ρ_z^f, and of free monovalent ions, ρ_1^f, are related to the number of condensed ions since the total number of ions within the cell is fixed:

$$\begin{aligned} \rho_z^f &\equiv (A - A_c)c_z^f = Ac_z - \rho_z, \\ \rho_1^f &\equiv (A - A_c)c_1^f = Ac_1 + \rho_{\mathrm{DNA}} - \rho_1 \end{aligned} \quad (6)$$

where we introduced the concentrations of free counterions c_z^f and c_1^f.

Finally, the electrostatic energy is evaluated as if all the bound ions are exactly at the cylinder rim, $r = d$, and the linearized Debye–Hückel approximation is used for the electrostatic potential at $r > d$. This leads to the last term in Eq. (4), where ϕ is the electrostatic potential at $r = d$, given by:

$$\phi = -2l_B(\rho_{\mathrm{DNA}} - z\rho_z - \rho_1)\frac{K_0(\kappa d)}{\kappa d K_1(\kappa d)} \quad (7)$$

where we assume that the outer cell radius is much larger than d and κ^{-1}, ρ_{DNA} is the number of unit charges per unit length of DNA, K_0 and K_1 are zeroth and first order modified Bessel functions of the first kind, respectively, and κ^{-1} is the Debye length:

$$\kappa^2 = 4\pi l_B\left[2c_1^f + z(z+1)c_z^f\right] \quad (8)$$

The number of condensed monovalent and z-valent counterions is found by minimizing the free energy with respect to ρ_1 and ρ_z, yielding:

Table 2
Comparison of two-phase models (two-phase, Manning) with PB theory. All the concentrations are in mM

c_1	$a\rho_z^*$	c_z^* (two-phase)	c_z^* (PB)	c_z^* (Manning)
2	0.194	4.1×10^{-4}	4.3×10^{-4}	7.5×10^{-7}
13	0.191	1.0×10^{-1}	3.7×10^{-2}	3.4×10^{-4}
23	0.173	7.4×10^{-2}	3.3×10^{-2}	4.1×10^{-4}
88	0.135	3.9×10^{-1}	1.1×10^{-1}	4.8×10^{-3}

$$\log\left(\frac{\rho_z}{c_z^f A_c}\right) = -z\phi; \quad \log\left(\frac{\rho_1}{c_1^f A_c}\right) = -\phi \quad (9)$$

4.2. Consequences for DNA aggregation

We are interested in the qualitative dependence of c_z^* on c_1. Note that c_z^* has the same role as c_z^f in the two-phase model. For the monovalent salt, assuming that $c_1 > c_{\mathrm{DNA}}$, c_1^f can be replaced by c_1 [7]. Eq. (9) then yields the following relation:

$$c_z^* = \frac{\rho_z^*}{A_c}\left(\frac{c_1 A_c}{\rho_1^*}\right)^z \quad (10)$$

where ρ_1^* is the linear density of bound monovalent ions at the onset of aggregation [14]. Qualitatively, ρ_1^* is the only ingredient that needs to be estimated in this equation, since c_1 is controlled experimentally and $z\rho_z^*$ is of order one.

The main outcome of Eq. (10) is that c_z^* scales roughly as $(c_1)^z$. This explains the large variation of c_z^* at different monovalent salt concentrations since $z = 4$. There are several sources for corrections to this scaling. The first one is the dependence of ρ_1^* on c_1 and ρ_z^*. A second source of corrections is the effect of short-range interactions, which was discussed in the previous section within PB theory. In addition, Eq. (10) involves all the approximations of the two-phase model.

4.3. Comparison with other models

We conclude this section by comparing the predictions of the two-phase model with those of PB theory and Manning's two-variable theory (see also Refs. [15,16]). This is instructive due to the wide use of two-phase models in the literature. Table 2 lists the value of c_z^* calculated with the two-phase model, using the values of c_1 and ρ_z^* of Table 1. The two-phase model can be seen to agree qualitatively with PB theory. Quantitatively, their predictions differ by a factor of up to four in the table.

Our two-phase model differs from Manning's two variable theory in some details. First, the area used in the expression for the entropy of bound counterions is different. Second, the expression for the electrostatic

energy of bound ions is given in Manning's theory by:

$$\phi = 2l_B(\rho_{\mathrm{DNA}} - z\rho_z - \rho_1)\log(1 - \mathrm{e}^{-\kappa a}). \quad (11)$$

Note that for small κd the two forms in Eqs. (7) and (11) are similar if d is replaced by a, since:

$$\frac{K_0(\kappa d)}{\kappa d K_1(\kappa d)} \simeq -\log(1 - \mathrm{e}^{-\kappa d}). \quad (12)$$

In the last column of Table 2 we present the results of Manning's two variable theory, in the version that was used in Refs. [12,13,16] (with different areas of condensation for monovalent and multivalent counterions). Compared to our two-phase model, deviations from PB theory are larger, typically of approximately two orders of magnitude. Since both two-phase models are quite similar to each other, their different predictions demonstrate the large sensitivity to model-dependent parameters. In our opinion such models are useful for obtaining qualitative predictions, but should be used with great care when quantitative predictions are required.

5. Summary

In this paper we discussed competition between ions of different valency in DNA aggregation, concentrating on DNA-counterion complexes in the dilute (non-aggregate) phase. Due to competition, the number of condensed multivalent ions is highly sensitive to salt concentration and to short-range, ion-specific effects. Simplified models that include only electrostatic interactions are thus limited in their capability to predict the conditions required for aggregation. An important experimental evidence for the importance of specific interactions is that different multivalent ions vary strongly in their ability to induce condensation or aggregation of DNA, even if they have the same valency [17,18]. In addition to the role of specific interactions in the dilute DNA phase, they also play a prominent role in the aggregates [20,21], where the gap between neighboring DNA chains is typically of order 10 Å [19].

Acknowledgments

We are grateful to E. Raspaud and J.-L. Sikorav for numerous discussions. Support from the US–Israel Binational Science Foundation (B.S.F.) under grant No. 287/02 and the Israel Science Foundation under grant No. 210/02 is gratefully acknowledged.

References

[1] Barrat JL, Joanny JF. Theory of polyelectrolyte solutions. Adv Chem Phys 1996;94:1–66.
[2] Manning GS. Limiting laws and counterion condensation in polyelectrolyte solutions: I. Colligative properties. J Chem Phys 1969;51:924–33.
[3] Manning GS. Limiting laws and counterion condensation in polyelectrolyte solutions: IV. The approach to the limit and the extraordinary stability of the charge fraction. Biophys Chem 1977;7:95–102.
[4] Boström M, Williams DRM, Ninham BW. The influence of ionic dispersion potentials on counterion condensation on polyelectrolytes. J Phys Chem 2002;106:7908–12.
[5] Rouzina I, Bloomfield VA. Influence of ligand spatial organization on competitive electrostatic binding to DNA. J Phys Chem B 1996;100:4305–13.
[6] Raspaud E, Olvera de la Cruz M, Sikorav J-L, Livolant F. Spermine-induced aggregation of DNA by polyamines: a polyelectrolyte behavior. Biophys J 1998;74:381–93.
[7] Burak Y, Ariel G, Andelman D. Onset of DNA aggregation in presence of monovalent and multivalent counterions. Biophys J 2003;85:2100–10.
[8] Korolev N, Lyubartsev AP, Laaksonen A, Nordenskiöld L. On the competition between water, sodium ions and spermine in binding to DNA: a molecular dynamics computer simulation study. Biophys J 2002;82:2860–75.
[9] Lyubartsev AP, Nordenskiöld L. Monte Carlo simulation study of DNA polyelectrolyte properties in the presence of multivalent polyamine ions. J Phys Chem B 1997;101:4335–42.
[10] Oosawa F. Polyelectrolytes. New York: Marcel Dekker, 1971.
[11] Manning GS. The molecular theory of polyelectrolyte solutions with applications to the electrostatic properties of polynucleotides. Q Rev Biophys II 1978;2:179–246.
[12] Wilson RW, Bloomfield VA. Counterion-induced condensation of deoxyribonucleic acid. A light scattering study. Biochemistry 1979;79:2192–6.
[13] Bloomfield VA, Wilson RW, Rau DC. Polyelectrolyte effects in DNA condensation by polyamines. Biophys Chem 1980;11:339–43.
[14] Rouzina I, Bloomfield VA. Competitive electrostatic binding of charged ligands to polyelectrolytes: planar and cylindrical geometries. J Phys Chem B 1995;100:4292–304 (For a more elaborate discussion see:).
[15] Belloni L, Drifford M, Turq P. Counterion diffusion in polyelectrolyte solutions. Chem Phys 1984;83:147–54.
[16] Wilson RW, Rau DC, Bloomfield VA. Comparison of polyelectrolyte theories of the binding of cations to DNA. Biophys J 1980;30:317–25.
[17] Deng H, Bloomfield VA. Structural effects of cobalt–amine compounds on DNA condensation. Biophys J 1999;77:1556–61.
[18] Saminathan M, Antony T, Shirahata A, Sigal LH, Thomas T, Thomas TJ. Ionic and structural specificity effects of natural and synthetic polyamines on the aggregation and resolubilization of single-, double- and triple-stranded DNA. Biochemistry 1999;38:3821–30.
[19] Pelta J, Livolant F, Sikorav J-L. DNA aggregation induced by polyamines and cobalthexamine. J Biol Chem 1996;271:5656–62.
[20] Rau DC, Parsegian VA. Direct measurement of the intermolecular forces between counterion-condensed DNA double helices. Biophys J 1992;61:246–59.
[21] Strey HH, Podgornik R, Rau DC, Parsegian VA. DNA–DNA interactions. Curr Opin Struct Biol 1998;8:309–13.